RSC Advances

PAPER

View Article Online
View Journal | View Issue

Cite this: *RSC Adv.*, 2026, **16**, 27692

Highly sensitive and selective electrochemical determination of curcumin using a polyaniline-based molecularly imprinted polymer

Amir Abbas Rafati *[a] and Esmaeil Karami[b]

A novel and highly selective electrochemical sensor based on a polyaniline molecularly imprinted polymer modified glassy carbon electrode (MIP–PANI/GCE) was developed for the determination of curcumin. The molecularly imprinted polymer was synthesized directly on the electrode surface *via* electropolymerization of aniline in the presence of curcumin as a template molecule, followed by template extraction to generate specific recognition sites. Cyclic voltammetry was employed to investigate the electrochemical behavior and polymer formation, while differential pulse voltammetry was used for the sensitive and quantitative determination of curcumin. Key experimental parameters affecting the sensor performance, including solution pH, polymerization conditions, and curcumin concentration, were optimized. Under optimal conditions, the MIP–PANI/GCE electrode exhibited a significantly enhanced electrochemical response toward curcumin compared to the corresponding non-imprinted polymer (NIP) electrode, confirming the successful formation of selective binding cavities. The sensor demonstrated a wide linear dynamic range, low detection limit, good repeatability, and satisfactory regeneration capability. Moreover, high selectivity toward curcumin was achieved in the presence of potential interfering substances, highlighting the effectiveness of the molecular imprinting strategy. The proposed MIP-based electrochemical sensor combines simplicity of fabrication, low cost, and excellent analytical performance, making it a promising alternative to conventional analytical techniques for the sensitive and selective determination of curcumin in food, pharmaceutical, and related real samples.

Received 12th April 2026
Accepted 18th May 2026

DOI: 10.1039/d6ra03086f

rsc.li/rsc-advances

1 Introduction

Curcumin (diferuloylmethane) is a naturally occurring polyphenolic compound extracted from the rhizome of *Curcuma longa* (turmeric). Pharmacologically curcumin, whose molecular structure is presented in Scheme 1, is also well known for its various medicinal properties.

At the optimized pH (~7), the enol form of curcumin predominates and is preferentially recognized by the MIP cavities due to enhanced hydrogen bonding interactions. Owing to its broad spectrum of biological and pharmacological activities—including anti-inflammatory, antioxidant, anticancer, antiviral, and antibacterial effects—curcumin has attracted significant attention in recent years from both academic and industrial communities.[1–5] Structurally, curcumin contains two phenolic moieties and a β-diketone group, which enable strong interactions with reactive oxygen species, metal ions, and biomolecules. These structural features not only underpin its biological activity but also render curcumin electrochemically active, making it a suitable target for electroanalytical detection.

Due to its extensive use in food, pharmaceutical, and nutraceutical products, accurate and selective determination of curcumin in complex matrices is of considerable importance. Conventional analytical techniques such as high-performance liquid chromatography (HPLC), thin-layer chromatography (TLC), and UV-vis spectrophotometry have been widely employed for curcumin analysis.[6–9] Despite their reliability, these methods often suffer from several drawbacks, including time-consuming procedures, expensive instrumentation, and the need for elaborate sample pretreatment. Consequently, the development of rapid, cost-effective, and highly selective analytical approaches for curcumin detection remains a significant challenge.

In recent years, molecularly imprinted polymers (MIPs) have emerged as powerful artificial recognition materials capable of selectively binding target molecules through tailor-made cavities complementary in shape, size, and functional groups.[10] Compared to biological recognition elements such as antibodies or enzymes, MIPs offer notable advantages including high chemical stability, low cost, long shelf life, and resistance to harsh environmental conditions.[11–16] These characteristics

[a]*Department of Physical Chemistry Faculty of Chemistry and Petroleum Sciences, Bu-Ali Sina University, P.O.Box 65174, Hamedan, Iran. E-mail: aa_rafati@basu.ac.ir; rafati_aa@yahoo.com; Tel: +98 81 3140 8080*

[b]*Clinical Biomechanics and Ergonomics Research Center, Aja University of Medical Sciences, Tehran, Iran*

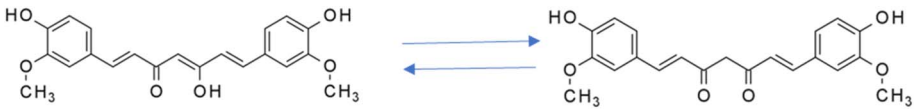

Scheme 1 Enol–keto tautomerism of curcumin.

make MIPs particularly attractive for sensing applications in complex real samples.

Among various fabrication strategies, the integration of MIPs with electrochemical transducers has proven to be an effective approach for enhancing both sensitivity and selectivity. In MIP-based electrochemical sensors, a thin imprinted polymer film is formed directly on the electrode surface, allowing efficient electron transfer and rapid target recognition. Electrodes such as glassy carbon electrodes (GCEs) modified with MIP layers exhibit increased effective surface area, a higher density of active binding sites, and improved analytical performance. Electrochemical techniques including cyclic voltammetry (CV), differential pulse voltammetry (DPV), and square wave voltammetry (SWV) are commonly employed to evaluate the sensing performance of these systems due to their high sensitivity and simplicity.[17–25]

Electropolymerization is one of the most advantageous methods for MIP fabrication on electrode surfaces, as it enables precise control over film thickness, morphology, and binding site distribution. Conducting polymers such as polyaniline (PANI) are particularly suitable for this purpose due to their excellent electrical conductivity, ease of synthesis, and strong adherence to electrode substrates. By electropolymerizing aniline in the presence of curcumin as a template molecule, a conductive MIP film with selective recognition sites can be generated, offering an efficient platform for curcumin detection.

The electrochemical response of MIP-based sensors is strongly influenced by experimental parameters such as solution pH, monomer-to-template ratio, polymerization conditions, scan rate, and template extraction time. Optimization of these parameters is essential to achieve maximum sensitivity, selectivity, and reproducibility of the sensor response.[16,26,27] In particular, the protonation state of curcumin and the polymer matrix plays a crucial role in governing adsorption behavior and electron-transfer kinetics at the electrode interface.

The present study focuses on the development of a novel electrochemical sensor based on a polyaniline molecularly imprinted polymer modified glassy carbon electrode (MIP–PANI/GCE) for the selective determination of curcumin. The proposed sensor combines the high selectivity of MIP recognition with the excellent electrochemical properties of PANI, enabling sensitive and reliable detection of curcumin in aqueous media. The analytical performance of the sensor is systematically evaluated through comparison with a non-imprinted polymer (NIP) electrode, optimization of key experimental parameters, and investigation of selectivity, repeatability, and regeneration capability. The results demonstrate that the developed MIP-based electrochemical sensor represents a promising alternative to conventional analytical methods for curcumin determination in food, pharmaceutical, and related applications.

2 Materials and methods

2.1 Chemicals and reagents

Curcumin (≥99%), aniline monomer, potassium ferricyanide $K_3[Fe(CN)_6]$, potassium ferrocyanide $K_4[Fe(CN)_6]$, potassium chloride (KCl), sulfuric acid (H_2SO_4), sodium hydroxide (NaOH), and ethanol were purchased from commercial suppliers and used without further purification. All aqueous solutions were prepared using double-distilled water. Phosphate buffer solutions (PBS) with different pH values were prepared and used as the supporting electrolyte throughout the experiments.

2.2 Apparatus and electrochemical measurements

Electrochemical measurements were carried out using a conventional three-electrode system connected to a potentiostat/galvanostat. A glassy carbon electrode (GCE, diameter 3 mm) served as the working electrode, while a platinum wire and an Ag/AgCl electrode were employed as the counter and reference electrodes, respectively. Cyclic voltammetry (CV) and

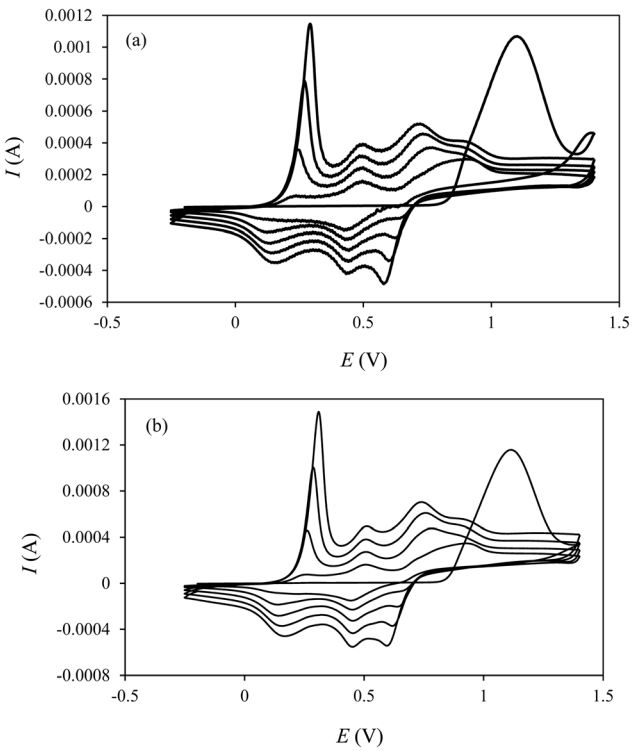

Fig. 1 Electropolymerization of aniline on GCE by cyclic voltammetry: (a) NIP–PANI/GCE in the absence of curcumin and (b) MIP–PANI/GCE in the presence of curcumin.

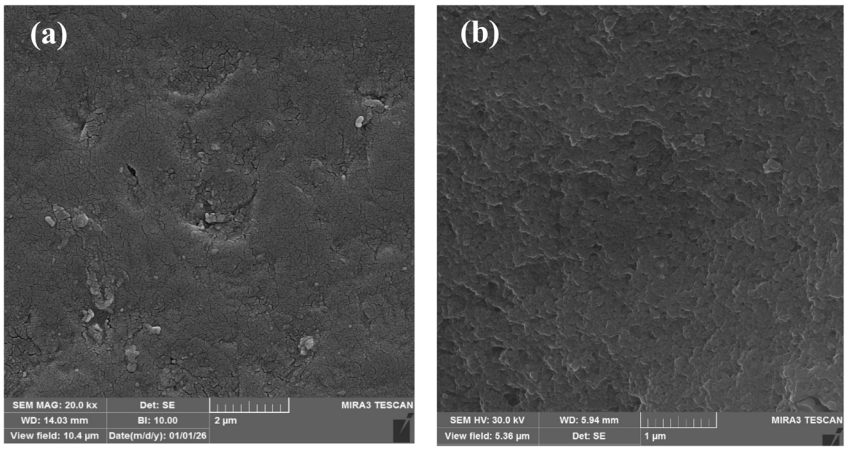

Fig. 2 SEM images of (a) bare GCE and (b) MIP–PANI/GCE after electropolymerization, confirming successful deposition of the polymer film on the electrode surface.

differential pulse voltammetry (DPV) were used to investigate the electrochemical behavior and analytical performance of the sensor. All experiments were conducted at room temperature.

2.3 Preparation of the bare glassy carbon electrode

Prior to modification, the GCE surface was mechanically polished with alumina slurry (0.05 μm) on a polishing cloth to obtain a mirror-like surface. The electrode was then rinsed thoroughly with distilled water and ultrasonically cleaned successively in ethanol and distilled water for 5 min each to remove any residual contaminants. The cleaned electrode was dried under ambient conditions before further modification.

2.4 Fabrication of the MIP–PANI/GCE modified electrode

The molecularly imprinted polymer was synthesized on the surface of the GCE by electropolymerization of aniline in the presence of curcumin as the template molecule. Typically, electropolymerization was performed in an acidic aqueous solution containing aniline monomer and a known concentration of curcumin. Electropolymerization was carried out by cyclic voltammetry in the potential range of −0.2 to +1.0 V (*vs.* Ag/AgCl) at a scan rate of 50 mV s^{-1} for 10 consecutive cycles, resulting in the formation of a thin PANI film on the electrode surface. These conditions were selected to ensure controlled film thickness and uniform polymer growth. After polymerization, the electrode was rinsed with distilled water to remove loosely bound species. The template was removed using a mixture of ethanol/acetic acid (9 : 1, v/v) under continuous stirring for 30 minutes. The template molecules were subsequently extracted from the polymer matrix by immersing the electrode in an appropriate solvent system under stirring until no further electrochemical signal of curcumin was observed. This process generated specific recognition cavities complementary to curcumin in terms of size, shape, and functional groups. For comparison, a non-imprinted polymer (NIP) electrode was prepared using the same procedure but in the absence of curcumin.

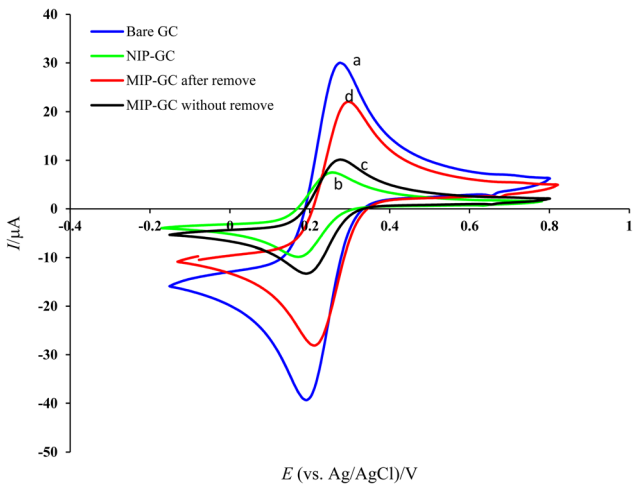

Fig. 3 Cyclic voltammograms of (a) bare GCE, (c) MIP–PANI/GCE before template removal, (d) MIP–PANI/GCE after template removal, and (b) NIP–PANI/GCE recorded in 5.0 mM $[Fe(CN)_6]^{3-/4-}$ containing 0.1 M KCl.

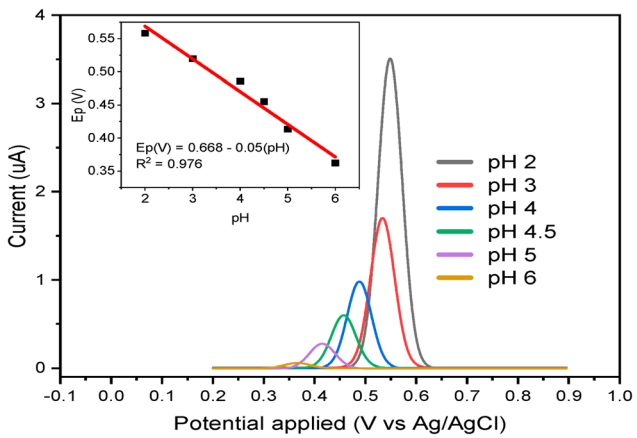

Fig. 4 Effect of solution pH on the DPV response of curcumin at the MIP–PANI/GCE.

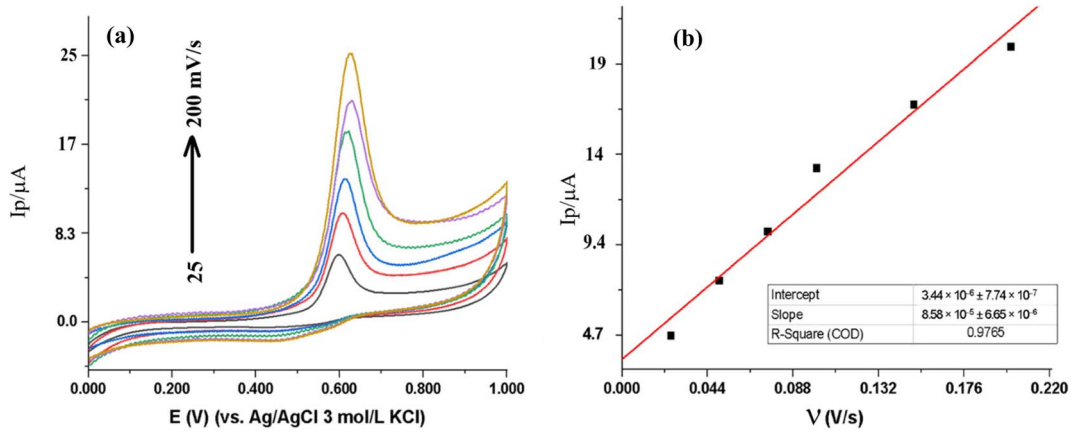

Fig. 5 (a) Cyclic voltammograms recorded at different scan rates; (b) linear dependence of peak current *versus* square root of scan rate.

2.5 Electrochemical characterization of the modified electrodes

The electrochemical properties of the bare GCE, MIP–PANI/GCE, and NIP–PANI/GCE were evaluated using cyclic voltammetry in a solution containing 5.0 mM $[Fe(CN)_6]^{3-/4-}$ and 0.1 M KCl as a redox probe. Changes in peak current and peak-to-peak separation were used to assess the successful modification and template removal processes.

2.6 Analytical procedure for curcumin determination

For curcumin determination, the MIP–PANI/GCE modified electrode was incubated in curcumin solutions of different concentrations prepared in PBS under optimized conditions. After an appropriate accumulation time, the electrode was rinsed gently with distilled water to remove non-specifically adsorbed molecules. Differential pulse voltammetry was then recorded in fresh supporting electrolyte to obtain the analytical signal. Calibration curves were constructed by plotting the peak current against curcumin concentration.

2.7 Selectivity, repeatability, and regeneration studies

The selectivity of the proposed sensor was evaluated by examining its response to curcumin in the presence of potential interfering substances. Repeatability was assessed by performing successive measurements using the same electrode, while reproducibility was evaluated using independently prepared MIP–PANI/GCE electrodes. Regeneration capability was investigated by removing bound curcumin from the electrode surface using the extraction solvent and reusing the sensor for multiple detection cycles.

3 Results and discussion

3.1 Electropolymerization of the MIP–PANI film

The electropolymerization behavior of aniline on the glassy carbon electrode surface was investigated by cyclic voltammetry

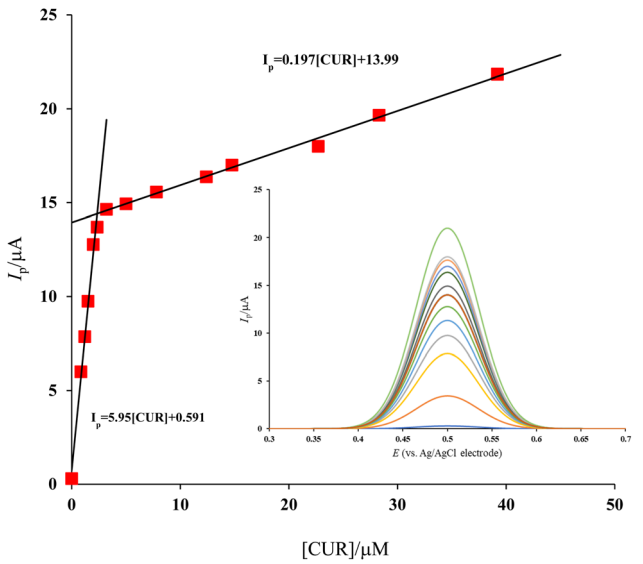

Fig. 6 The calibration curve based on I_p *versus* concentration of curcumin (inset graph is the DPV responses of the MIP–PANI/GCE to different curcumin concentrations).

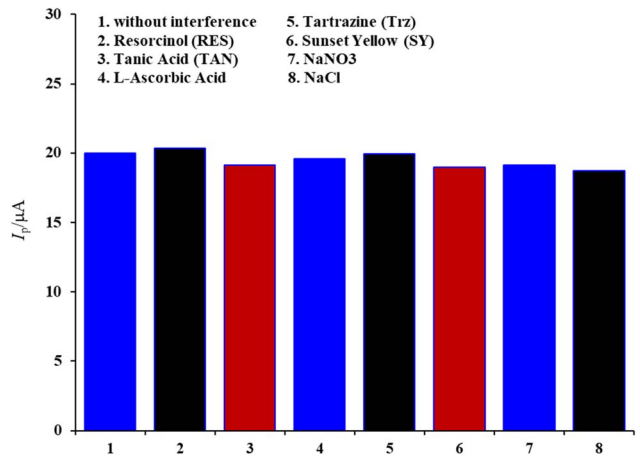

Fig. 7 Relative signal variation (%) of curcumin in the presence of various interfering species, showing less than 8% deviation compared to the target analyte.

Table 1 Determination of curcumin in real samples

Sample type	Added (μM)	Found (μM)	Recovery (%)	RSD (%)
Turmeric powder	5.0	5.12	102.4	3.2
	10.0	9.68	96.8	2.9
	20.0	20.7	103.5	3.5
Pharmaceutical capsule	5.0	4.92	98.4	2.7
	10.0	10.3	103.0	3.1
	20.0	19.6	98.0	2.8

in the presence and absence of curcumin. As shown in Fig. 1, successive potential cycles led to a gradual increase in redox current, indicating the continuous growth of a conductive polyaniline film.

The molar ratio of aniline to curcumin plays a crucial role in determining the structure and efficiency of the imprinted polymer. In this work, the selected ratio was chosen to provide a balance between sufficient template incorporation and the formation of a conductive polymer network. It is well established that excessive template concentration may hinder polymer growth and reduce conductivity, whereas insufficient template content can lead to poorly defined recognition sites. Therefore, an optimized intermediate ratio was employed, consistent with previously reported MIP-based electrochemical systems, to ensure effective cavity formation and satisfactory sensor performance.

In the presence of curcumin, the polymerization current was noticeably lower than that of the non-imprinted system. This behavior can be attributed to the incorporation of curcumin molecules within the polymer matrix, which partially restricts charge transport and polymer chain propagation. Such suppression is commonly observed during molecular imprinting and provides strong evidence for the successful entrapment of the template molecules within the growing polymer network.

SEM characterization was carried out to investigate the surface morphology of the electrodes before and after electropolymerization. As shown in Fig. 2a, the bare glassy carbon electrode exhibited a relatively smooth and homogeneous surface morphology. After electropolymerization and formation of the MIP–PANI layer, significant morphological changes were observed (Fig. 2b). The modified electrode surface became rougher and more heterogeneous, showing granular and clustered polymeric structures distributed over the electrode surface, confirming successful deposition of the molecularly imprinted polyaniline film. The porous morphology of the polymer layer can provide a larger effective surface area and facilitate analyte diffusion toward the imprinted recognition sites, which is beneficial for improving the electrochemical response of the sensor.

3.2 Electrochemical characterization using redox probe

The electrochemical properties of the bare GCE, MIP–PANI/GCE before template removal, MIP–PANI/GCE after template removal, and NIP–PANI/GCE were evaluated using the $[Fe(CN)_6]^{3-/4-}$ redox probe.

As illustrated in Fig. 3, the bare GCE exhibited sharp and reversible redox peaks, indicative of fast electron-transfer kinetics. After polymer deposition, a significant decrease in peak current was observed due to the insulating nature of the polymer layer. Notably, after template extraction, the MIP–PANI/GCE electrode showed a partial recovery of peak current compared to the NIP electrode, confirming the formation of accessible recognition cavities that facilitate ion diffusion and electron transfer.

Although surface characterization techniques such as SEM or AFM were not employed in this study, the successful formation of the MIP–PANI film and the removal of template molecules can be clearly inferred from electrochemical results. The observed decrease in redox peak current after polymer deposition, followed by its partial recovery after template extraction, provides strong evidence for the formation of a polymer layer with accessible recognition cavities. Moreover, the improved analytical performance of the MIP–PANI/GCE modified electrode compared to the non-imprinted polymer further confirms the effectiveness of the imprinting process. Nevertheless, future studies will include morphological characterization to provide direct visualization of the polymer structure.

3.3 Effect of solution pH

The influence of solution pH on the electrochemical response of curcumin was systematically investigated. As depicted in Fig. 4, the peak current increased with increasing pH up to an optimal value (typically near neutral pH), after which a decline was observed.

This trend reflects the combined effect of curcumin protonation state and the conductivity of polyaniline. At low pH values, excessive protonation reduces the interaction between curcumin and the imprinted cavities, while at higher pH values, the dedoping of PANI leads to decreased conductivity. Therefore, the selected optimal pH represents a compromise between molecular recognition efficiency and charge-transfer capability.

3.4 Scan rate study and kinetic analysis

The effect of scan rate on the oxidation peak current of curcumin was investigated by cyclic voltammetry. As shown in Fig. 5a, the peak current increased with increasing scan rate. A linear relationship between peak current and the square root of scan rate (Fig. 5b) indicates that the electrochemical process is predominantly diffusion-controlled.

Table 2 Repeatability, reproducibility, and regeneration performance

Parameter	RSD (%)
Repeatability ($n = 5$)	3.1
Reproducibility ($n = 4$)	4.2
After 5 regeneration cycles	6.0

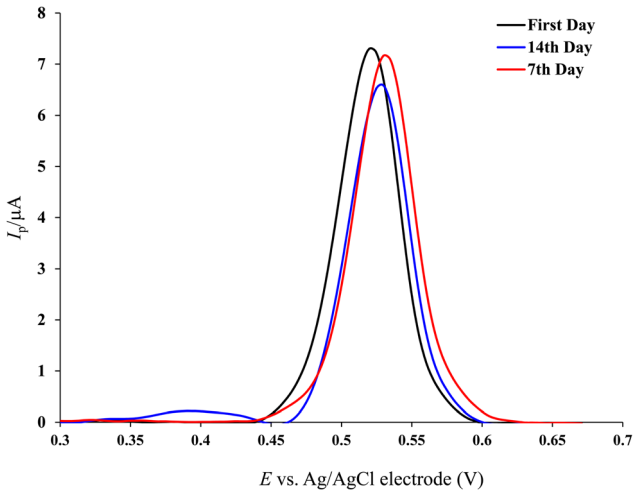

Fig. 8 Stability study of MIP–PANI/GCE sensor towards determination of 5 μM of curcumin.

The slight shift in peak potential with increasing scan rate suggests quasi-reversible electron-transfer kinetics. These results confirm that curcumin molecules bound within the imprinted sites remain electrochemically active and accessible.

3.5 Analytical performance and calibration curve

DPV was selected for quantitative analysis of curcumin due to its higher sensitivity and better signal resolution compared to cyclic voltammetry.

As shown in Fig. 6 (inset graph), the oxidation peak current increased proportionally with curcumin concentration. The corresponding calibration curve (Fig. 6) exhibited excellent linearity over a wide concentration range.

The limit of detection (LOD), calculated based on a signal-to-noise ratio of 3, demonstrates the high sensitivity of the proposed sensor. In contrast, the NIP–PANI/GCE electrode showed a much weaker response, confirming the decisive role of molecular imprinting in signal enhancement.

Two linear regression equations were obtained corresponding to different concentration ranges:

$$I_p(\mu A) = 5.95[CUR/(\mu M)] + 0.591 \ (R^2 = 0.991)$$

$$I_p(\mu A) = 0.197[CUR/(\mu M)] + 13.99 \ (R^2 = 0.995)$$

The limit of detection (LOD) and the limit of quantification (LOQ) values were obtained as 0.37 nM and 1.23 nM, respectively.

It should be noted that the calculated limit of detection (LOD) does not necessarily coincide with the lower limit of the linear dynamic range. The LOD represents the minimum detectable concentration based on the signal-to-noise ratio (S/N = 3), whereas the linear range corresponds to the concentration interval over which the sensor response is directly proportional to analyte concentration. In this study, although detectable signals were observed at nanomolar levels, the linear calibration range begins at higher concentrations where the response exhibits good linearity and reproducibility. Therefore, low-concentration data points were not included in the linear regression analysis.

3.6 Selectivity study

The selectivity of the MIP–PANI/GCE sensor was evaluated by comparing its response to curcumin with that of potential interfering species. The influence of various organic and inorganic compounds commonly found in pharmaceutical and biological samples on the quantification of curcumin at the MIP–PANI/GCE was investigated. Compounds such as resorcinol (RES), tannic acid (TAN), L-ascorbic acid (L-AA), tatrazine (Trz), sunset yellow (SY), $NaNO_3$ and NaCl were added to pH 7.0 PBS in the presence of 30 μM curcumin at a concentration of 3 mM of interferences, using the DPV technique. The results indicate that the presence of interfering species caused a signal variation of less than 8%, demonstrating the high selectivity of the proposed sensor (Fig. 7), thereby validating its applicability

Table 3 Electrochemical sensors for curcumin detection, presented in decreasing order of LOD

Modified electrode	Matrix	Detection technique	Linear range	Detection limit	Reference
HMDE	—	DPASV	4.95×10^{-7}–2.76×10^{-5} M	—	28
SPCE	40% ethanol	ASV	2.2×10^{-6}–7×10^{-5} M	4.9×10^{-6} M	29
rGO-CPE	Human blood serum	CV	1.0×10^{-5}–6.0×10^{-3} M	3.183×10^{-6} M	30
MWCNTs-BPPGE	Turmeric powder	ASV	2.0×10^{-6}–1.0×10^{-4} M	0.45×10^{-6} M	31
PTY-CPE	Food supplement (liquid)	CV	2.0×10^{-6}–1.0×10^{-5} M	1.1×10^{-6} M	32
CQDs/GCE	Turmeric powder	DPV	6.0×10^{-8}–4.0×10^{-5} M	3.0×10^{-8} M	33
$NiCl_2$/GCE	Human blood serum	DPV	1.0×10^{-5}–6.0×10^{-4} M	1.09×10^{-7} M	34
CNTs-CMC	Food samples	CV	1.0×10^{-6}–4.8×10^{-5} M	8.4×10^{-8} M	35
poly(L-Cys) MIP/ $CuCo_2O_4$/N-CNTs/ PGO/GCE	Serum sample	DPV	1.0×10^{-7}–1.0×10^{-6} 1.0×10^{-6}–3.0×10^{-5} M	3.0×10^{-8} M	36
Gr/GCE	*Curcuma longa* L.	LSV	5.0×10^{-8}–3.0×10^{-6} M	3.0×10^{-8} M	37
MIP-CPE	Curcuma powder, curcuma cookies	CV	1.0×10^{-7}–5.0×10^{-5} M	1.0×10^{-8} M	38
PANI-MIP/MWCNTs/GC (this work)	—	DPV	1.0×10^{-6}–4.0×10^{-5} M	3.7×10^{-10} M	This work

for determining curcumin in pharmaceutical and urine samples.

3.7 Real sample analysis

To evaluate the practical applicability of the proposed MIP–PANI/GCE sensor, its performance was investigated in real samples, including turmeric powder and a commercial pharmaceutical formulation containing curcumin.

3.7.1 Sample preparation

3.7.1.1 Turmeric sample. A known amount of turmeric powder (0.50 g) was accurately weighed and transferred into a 50 mL flask. Then, 20 mL of an ethanol–water mixture (70 : 30, v/v) was added as the extraction solvent. The mixture was sonicated for 30 minutes to ensure efficient extraction of curcumin, followed by centrifugation at 4000 rpm for 10 minutes. The supernatant was filtered and appropriately diluted with phosphate buffer solution (PBS, pH 7.0) prior to electrochemical analysis.

3.7.1.2 Pharmaceutical sample. A commercial curcumin capsule was opened, and an accurately weighed portion equivalent to one capsule content was dissolved in 25 mL of ethanol. The solution was sonicated for 20 minutes and filtered to remove insoluble excipients. The filtrate was diluted with PBS (pH 7.0) to obtain suitable concentrations within the linear range of the sensor.

3.7.2 Recovery study. The accuracy of the method was assessed using a standard addition method. Known amounts of curcumin standard solution were spiked into the pre-analyzed real samples at three different concentration levels. The spiked samples were then analyzed using differential pulse voltammetry under optimized conditions. The recovery (%) was calculated using the following equation:

$$\text{Recovery}(\%) = \frac{\text{Found amount} - \text{Original amount}}{\text{Added amount}} \times 100$$

The obtained results are summarized in Table 1. The recoveries for curcumin in both turmeric and pharmaceutical samples were found to be in the range of 96.8% to 103.5%, with relative standard deviation (RSD) values lower than 4.0%.

These results demonstrate (i) high accuracy of the proposed sensor, (ii) negligible matrix interference and (iii) good reliability in complex real samples. The slightly varying recovery values can be attributed to minor matrix effects; however, they remain within acceptable analytical limits.

The successful determination of curcumin in real samples confirms that the developed MIP–PANI/GCE sensor is suitable for practical applications in food and pharmaceutical analysis. The combination of high selectivity, sensitivity, and simple sample preparation highlights its potential as an alternative to conventional analytical techniques.

3.8 Repeatability, reproducibility, stability and regeneration

The repeatability and reproducibility of the proposed sensor were evaluated, and the results are summarized in Table 2. Low relative standard deviation (RSD) values indicate excellent stability and fabrication reproducibility. Additionally, the sensor retained most of its initial response after several regeneration cycles, highlighting its practical applicability.

Although long-term storage stability of the sensor was not systematically evaluated in this study, the obtained results for repeatability, reproducibility, and regeneration indicate that the MIP–PANI/GCE modified electrode exhibits good operational stability. The low RSD values and the retention of sensor response after multiple regeneration cycles suggest that the polymer film maintains its structural integrity and binding capability. Furthermore, molecularly imprinted polymers are generally known for their high chemical stability and resistance to environmental variations. Nevertheless, a comprehensive investigation of long-term storage stability over extended periods will be carried out in future work.

The long-term storage stability of the fabricated MIP–PANI/GCE sensor was investigated over a period of 14 days. The modified electrode was stored under ambient laboratory conditions, and its electrochemical response toward curcumin was periodically monitored using DPV measurements. As shown in Fig. 8, the sensor retained approximately 92% of its initial current response after 14 days, demonstrating acceptable long-term stability and preservation of the imprinted recognition sites. The slight decrease in signal intensity may be attributed to gradual surface aging or partial loss of active binding sites over time. These results indicate that the proposed sensor possesses suitable storage stability for practical electrochemical applications.

3.9 Comparison with reported curcumin sensors

A comparison between the proposed sensor and previously reported electrochemical methods is presented in Table 3. The MIP–PANI/GCE exhibits competitive or superior analytical performance while offering a simpler fabrication strategy.

4 Conclusion

In this study, a molecularly imprinted electrochemical sensor based on a polyaniline-modified glassy carbon electrode (CUR–MIP/PANI/GCE) was successfully developed for the selective detection of curcumin. The MIP film was prepared *via* electropolymerization of aniline in the presence of curcumin as the template, resulting in the formation of specific recognition sites after template removal.

Electrochemical measurements using differential pulse voltammetry revealed that the MIP–PANI/GCE modified electrode exhibited a significantly enhanced oxidation current compared to the non-imprinted polymer. Under optimized conditions, the sensor showed a linear response toward curcumin over the concentration range of 1–40 μM, with a low limit of detection of 0.37 nM. The proposed sensor demonstrated excellent selectivity, with less than 5–10% signal variation in the presence of high concentrations of potential interfering species. Moreover, good repeatability (RSD < 3%) and satisfactory regeneration performance were achieved, confirming the stability and reusability of the sensor.

Overall, the CUR–MIP/PANI/GCE sensor provides a simple, low-cost, and sensitive platform for curcumin determination and represents a promising alternative to conventional analytical methods for applications in food and pharmaceutical analysis.

Author contributions

Amir Abbas Rafati: project administration, conceptualization, supervision, funding acquisition, writing – review & editing, resource, validation. Esmaeil Karami: investigation, methodology, visualization, writing – original draft, data curation, formal analysis, software, data interpretation, reviewed and edited the manuscript. All authors read and approved the final manuscript.

Conflicts of interest

The author declares no conflicts of interest.

Data availability

All data supporting the findings of this study are available from the corresponding author upon reasonable request.

Acknowledgements

The authors greatly acknowledge Bu-Ali Sina University for providing laboratory facilities and institutional support.

References

1 K. Kaur, A. K. Al-Khazaleh, D. J. Bhuyan, F. Li and C. G. Li, *Antioxidants*, 2024, **13**, 1092, DOI: 10.3390/antiox13091092.
2 J. Sharifi-Rad, *et al.*, *Front. Pharmacol*, 2020, **11**, 1021, DOI: 10.3389/fphar.2020.01021.
3 S. Fuloria, *et al.*, *Front. Pharmacol*, 2022, **13**, 820806, DOI: 10.3389/fphar.2022.820806.
4 M. Anas, A. Falak, A. Khan, W. A. Khattak, S. Gul Nisa, Q. Aslam, K. A. Khan, M. H. Saleem, S. Fahad and J. Umm, *Al-Qura Univ. Appl. Sci.*, 2024, 1–16, DOI: 10.1007/s43994-024-00200-7.
5 A. Amalraj, A. Pius and S. Gopi, *J. Tradit. Complement. Med.*, 2017, **7**, 205–233, DOI: 10.1016/j.jtcme.2016.05.005.
6 V. S. R. Kotra, S. Latha and T. K. Goswami, *J. Food Sci. Technol.*, 2019, **56**, 5153–5166, DOI: 10.1007/s13197-019-03986-1.
7 A. B. Sravani, E. M. Mathew, V. Ghate and S. A. Lewis, *J. Fluoresc.*, 2022, **32**, 1517–1527, DOI: 10.1007/s10895-022-02947-w.
8 P. Kushwaha, B. Shukla, J. Dwivedi and S. Saxena, *J. Pharm. Sci.*, 2021, **7**, 178, DOI: 10.1186/s43094-021-00330-3.
9 E. Jara-Cornejo, E. Peña-Bedón, M. Torres-Moya, S. Espinoza, M. D. P. T. Sotomayor, G. Picasso, J. C. Tuesta, R. López and S. Khan, *Polymers*, 2024, **16**, 366, DOI: 10.3390/polym16030366.
10 L. Chen, X. Wang, W. Lu, X. Wu and J. Li, *Chem. Soc. Rev.*, 2016, **45**, 2137–2211, DOI: 10.1039/C6CS00061D.
11 X. Liu, L. Zhu, X. Gao, Y. Wang, H. Lu, Y. Tang and J. Li, *Food Chem.*, 2016, **202**, 309–315, DOI: 10.1016/j.foodchem.2016.02.015.
12 A. Ostovan, M. Arabi, Y. Wang, J. Li, B. Li, X. Wang and L. Chen, *Adv. Mater.*, 2022, **34**, 2203154, DOI: 10.1002/adma.202203154.
13 K. Haupt and K. Mosbach, *Chem. Rev.*, 2000, **100**, 2495–2504, DOI: 10.1021/cr990099w.
14 S. He, L. Zhang, S. Bai, H. Yang, Z. Cui, X. Zhang and Y. Li, *Eur. Polym. J.*, 2021, **143**, 110179, DOI: 10.1016/j.eurpolymj.2020.110179.
15 L. Ye and K. Mosbach, *Chem. Mater.*, 2008, **20**, 859–868, DOI: 10.1021/cm703190w.
16 L. Wang, M. Pagett and W. Zhang, *Sens. Acutators Rep.*, 2023, **5**, 100153, DOI: 10.1016/j.snr.2023.100153.
17 S. A. Piletsky and A. P. F. Turner, *Electroanalysis*, 2002, **14**, 317–323, DOI: 10.1002/1521-4109.
18 M. I. Pilo, G. Sanna and N. Spano, *Chemosensors*, 2024, **12**, 81, DOI: 10.3390/chemosensors12050081.
19 B. Lakard, *Appl. Sci.*, 2020, **10**, 6614, DOI: 10.3390/app10186614.
20 E. Katz and I. Willner, *Electroanalysis*, 2003, **15**, 913–947, DOI: 10.1002/elan.200390114.
21 J. Wang, *Biosens. Bioelectron.*, 2006, **21**, 1887–1892, DOI: 10.1016/j.bios.2005.10.027.
22 H. Zeng, Y. Xie, T. Liu, Z. Chu, E. Dempsey and W. Jin, *Sens. Diagn.*, 2024, **3**, 165–180, DOI: 10.1039/D3SD00160A.
23 M. Shekari, S. Moghari, E. A. Dawi and H. A. Khonakdar, *Polym. Adv. Technol.*, 2025, **36**, e70293, DOI: 10.1002/pat.70293.
24 D. Nevoltris and R. Ollier, *Antibody Engineering: Methods and Protocols*, Humana, New York, NY, 2018, 1–22.
25 B. Sellergren, *Molecularly Imprinted Polymers: Man-Made Mimics of Antibodies and Their Applications in Analytical Chemistry*, Elsevier, 2001.
26 A. A. Lahcen, K. Saidi and A. Amine, *Curr. Opin. Electrochem.*, 2025, **54**, 101752, DOI: 10.1016/j.coelec.2025.101752.
27 M. Díaz-Álvarez, E. Turiel and A. Martín-Esteban, *J. Sep. Sci.*, 2023, **46**, 2300157, DOI: 10.1002/jssc.202300157.
28 Z. Stanić, A. Voulgaropoulos and S. Girousi, *Electroanalysis*, 2008, **20**, 1263–1266, DOI: 10.1002/elan.200804177.
29 D. M. Wray, C. Batchelor-McAuley and R. G. Compton, *Electroanalysis*, 2012, **24**, 2244–2248, DOI: 10.1002/elan.201200560.
30 M. Rahimnejad, R. Zokhtareh, A. A. Moghadamnia and M. Asghary, *Port. Electrochim. Acta*, 2020, **38**, 29–42, DOI: 10.4152/pea.202001029.
31 K. Chaisiwamongkhol, K. Ngamchuea, C. Batchelor-McAuley and R. G. Compton, *Electroanalysis*, 2017, **29**, 1049–1055, DOI: 10.1002/elan.201600670.
32 E. S. D'Souza, J. G. Manjunatha, C. Raril, G. Tigari, H. J. Arpitha and S. Shenoy, *Surfaces*, 2021, **4**, 191–204, DOI: 10.3390/surfaces4030017.

33 R. M. Shereema, T. P. Rao, V. B. Sameer Kumar, *et al.*, *Mater. Sci. Eng., C*, 2018, **93**, 21–27, DOI: 10.1016/j.msec.2018.07.055.
34 R. Zokhtareh and M. Rahimnejad, *Electroanalysis*, 2018, **30**, 921–927, DOI: 10.1002/elan.201700770.
35 R. Wada, S. Takahashi, H. Muguruma and N. Osakabe, *Anal. Sci.*, 2020, **36**, 1113–1118, DOI: 10.2116/analsci.20P021.
36 A. Mohammadinejad, E. Abouzari-Lotf, G. Aleyaghoob, M. Rezayi and R. Kazemi Oskuee, *Food Chem.*, 2022, **386**, 132845, DOI: 10.1016/j.foodchem.2022.132845.
37 K. Li, Y. Li, L. Yang, L. Wang and B. Ye, *Anal. Methods*, 2014, **6**, 7801–7808, DOI: 10.1039/C4AY01492H.
38 Q. Zhou, H. Y. Zhai, Y. F. Pan and K. Li, *RSC Adv.*, 2017, **7**, 22913–22918, DOI: 10.1039/C7RA02253K.